A Letters Journal Exploring the Frontiers of Physics

March 2020

EPL, **129** (2020) 67001 www.epljournal.org
doi: 10.1209/0295-5075/129/67001

Superconductivity in Se-doped $La_2O_2Bi_2Pb_2S_{6-x}Se_x$ with a $Bi_2Pb_2Ch_4$-type thick conducting layer

Rajveer Jha, Yosuke Goto, Tatsuma D. Matsuda, Yuji Aoki and Yoshikazu Mizuguchi[(a)]

Department of Physics, Tokyo Metropolitan University - 1-1, Minami-osawa, 192-0397 Hachioji, Japan

received 13 February 2020; accepted in final form 9 April 2020
published online 23 April 2020

PACS 74.70.-b – Superconducting materials other than cuprates
PACS 74.62.Dh – Effects of crystal defects, doping and substitution
PACS 74.25.F- – Transport properties

Abstract – $La_2O_2Bi_2Pb_2S_6$ is a layered Bi-based oxychalcogenide with a thick four-layer–type conducting layer. Although $La_2O_2Bi_2Pb_2S_6$ is a structural analogue of $La_2O_2Bi_3AgS_6$, which is a superconductor, insulating behavior has been observed in $La_2O_2Bi_2Pb_2S_6$ at low temperatures, and no superconductivity has been reported. Herein, we demonstrate superconductivity in $La_2O_2Bi_2Pb_2S_{6-x}Se_x$ via partial substitution of Se in the S sites. Owing to the Se doping, the normal state electrical resistivity of $La_2O_2Bi_2Pb_2S_{6-x}Se_x$ at low temperatures was dramatically suppressed, and superconductivity was observed at a transition temperature (T_c) of 1.2 K for $x = 0.5$. T_c increased with increasing Se concentration: $T_c = 1.9$ K for $x = 1.0$. By applying high pressure for $x = 1.0$, bulk superconductivity was confirmed and the T_c increased up to 3.6 K at 0.89 GPa.

Copyright © EPLA, 2020

Introduction. – Layered compounds have been widely studied in the search for new superconductors since the discovery of (high-transition-temperature) high-T_c cuprates [1]. After the cuprates, Fe-based and $BiCh_2$-based superconductors (Ch: S and Se) have been discovered, and many others have been synthesized [2–5]. In those layered superconductors, the important structure is a superconducting layer commonly contained in the layer stacking: a CuO_2 layer in cuprates and an FeAs or FeSe layer in Fe-based superconductors [6–8]. In $BiCh_2$-based superconductors, a $BiCh_2$ layer is the basic superconducting layer [3–5].

Since the discovery of BiS_2-based superconductors, namely, $Bi_4O_4S_3$ and $La(O,F)BiS_2$, in 2012 [3,4], many related superconductors with BiS_2 [9–18], $BiSe_2$ [19,20], or $Bi(S,Se)_2$ superconducting layers [21–24] have been synthesized. The crystal structure of $BiCh_2$-based compounds has an interesting feature, that is, the presence of a van der Waals gap between two $BiCh_2$ layers. The space in this gap could be used to create new $BiCh_2$-type compounds with a thick conducting layer [25–27].

As studied in cuprates, stacking many conducting planes along the *c*-axis could be a promising way to achieve a higher T_c in a layered system [6,28,29]. Hence, layered oxychalcogenides, such as $La_2O_2M_4S_6$ (M: metals like Bi, Pb, Sn, and Ag), with a thicker *four-layer–type* conducting layer of M_4S_6 have been synthesized with the expectation of demonstrating a higher T_c than that observed in two-layer–type $BiCh_2$-based superconductors [25–27]. The four-layer–type $La_2O_2M_4S_6$ compounds typically have a tetragonal structure with a space group of $P4/nmm$. The structure can be regarded as a stacking of La_2O_2, BiS_2, M_2S_2, and BiS_2 layers in sequence [26]; a crystal structure image for M = Pb is displayed in fig. 1(d). A rock-salt–type M_2S_2 layer is inserted between two BiS_2 layers where a van der Waals gap would exist in a two-layer–type $LaOBiS_2$ (described as $La_2O_2Bi_2S_4$ for one unit cell). In fact, the outer layers are basically BiS_2 layers, and the inner rock-salt layer is occupied by M and S ions. From a structural viewpoint, the composition can be described as $La_2O_2Bi_2M_2S_6$.

Recently, we observed superconductivity with a T_c of 0.5 K in $La_2O_2Bi_3AgS_6$ (M = $Bi_{0.5}Ag_{0.5}$) [30]. Furthermore, we have studied the effects of doping on the superconductivity of the $La_2O_2Bi_3AgS_6$ system. Partial substitution of Ag by Sn increased T_c up to 2.5 K in $La_2O_2Bi_3Ag_{0.6}Sn_{0.4}S_6$ [31]. Additionally, partial Se substitution for S resulted in bulk superconductivity at 3.5 K in $La_2O_2Bi_3Ag_{0.6}Sn_{0.4}S_{5.7}Se_{0.3}$ [31]. T_c further increased up to 4.0 K with RE-site substitution in

[(a)]E-mail: mizugu@tmu.ac.jp

$La_{2-x}RE_xO_2Bi_3Ag_{0.6}Sn_{0.4}S_6$ (RE = Eu, Nd, and Pr) compounds [32,33]. Based on these recent developments with regard to new four-layer–type Bi-based superconductors, we found that the chemical pressure effect was useful for inducing bulk superconductivity in $La_2O_2Bi_2M_2S_6$ systems. The chemical pressure effect has been proposed as one of the essential parameters for the emergence of bulk superconductivity in typical $BiCh_2$-based compounds [14,21–24,34]. In the RE(O,F)$BiCh_2$ system, in-plane chemical pressure, which was tuned by RE-site and/or Ch-site substitutions, suppresses in-plane local disorder, which is unfavorable for the emergence of bulk superconductivity [35–39]. As mentioned previously, four-layer–type $La_2O_2Bi_2M_2S_6$ compounds are also sensitive to chemical pressure effects. Therefore, the chemical pressure could be useful for further exploration of new four-layer–type superconductors.

In this study, we have investigated the effects of substituting Se in the S sites in $La_2O_2Bi_2Pb_2S_6$, which was the first four-layer–type compound synthesized by Sun *et al.* and proposed as a promising thermoelectric material [25]. Although theoretical calculations suggested that $La_2O_2Bi_2Pb_2S_6$ is a metal [26], the obtained samples showed insulating behavior at low temperatures [25]. We have investigated the effects of partial substitutions of the Pb sites by Ag, Cd, In, Sn, and Sb, but all of the examined samples showed insulating characteristics at low temperatures. Therefore, in this study, we have investigated the effects of substituting Se in the S sites in $La_2O_2Bi_2Pb_2S_{6-x}Se_x$. Owing to the Se substitution, the insulating behavior was suppressed, and electrical resistivity that was apparently lower than that of pure $La_2O_2Bi_2Pb_2S_6$ was observed even at the lowest temperature of our system ($T = 0.4\,\mathrm{K}$). We observed superconductivity at $T_c = 1.2\,\mathrm{K}$ for $x = 0.5$ and $T_c = 1.9\,\mathrm{K}$ for $x = 1.0$.

Experimental details. – Polycrystalline samples of $La_2O_2Bi_2Pb_2S_{6-x}Se_x$ (x = 0, 0.5, and 1.0) were prepared by a solid-state reaction method. Powders of La_2S_3 (99.99%), Bi_2O_3 (99.9%), Pb (99.99%), and grains of Bi (99.999%), S (99.99%), and Bi_2Se_3 (pre-synthesized from Bi and Se) with a nominal composition of $La_2O_2Bi_2Pb_2S_{6-x}Se_x$ (x = 0, 0.5, and 1.0) were mixed using a pestle and a mortar, pelletized, sealed in an evacuated quartz tube, and heated at 690 °C for 15 h. The heated samples were reground, pelletized, and heated at 740 °C for 35 h. The optimal annealing conditions and the phase purity of the prepared samples were examined using laboratory X-ray diffraction (XRD) with a Cu-K_α radiation by a conventional θ-2θ method. To discuss the lattice structure, Rietveld analyses were performed with RIETAN-FP [40]. We assumed perfect site selectivity of Bi and Pb based on the previous structural analyses for $La_2O_2Bi_2Pb_2S_6$ [26]. As the obtained XRD intensity and profile were not sufficient for the determination of displacement parameters, we have performed refinements with fixed isotropic displacement parameters. A schematic image of the crystal structure was drawn using VESTA [41]. The actual composition of the synthesized samples was investigated by energy dispersive X-ray spectroscopy (EDX) on a scanning electron microscope SEM (TM-3030 (Hitachi)). The electrical resistivity down to $T = 0.5\,\mathrm{K}$ was measured by a four-probe method using a ^{3}He probe platform on the Physical Property measurement system (PPMS: Quantum Design). The Seebeck coefficient was measured by a four-probe method at room temperature on ZEM-3 (advance RIKO). The temperature dependence of the Hall coefficient was measured with a standard five-prove configuration on PPMS. The temperature dependence of magnetic susceptibility was measured by a SQUID (superconducting interference devise) magnetometer (MPMS3: Quantum Design) with an applied magnetic field of 1 mT. For high-pressure measurements, a piston-cylinder–type pressure cell was used. Applied pressure was estimated using a T_c of Pb.

Results and discussion. – Figure 1(a) shows room temperature powder XRD patterns for $La_2O_2Bi_2Pb_2S_{6-x}Se_x$ (x = 0, 0.5, and 1.0) compounds. The obtained samples are crystalized in a tetragonal crystal structure with a space group of $P4/nmm$. For all the samples, the main phase was $La_2O_2Bi_2Pb_2S_{6-x}Se_x$. As indicated by the symbol, a La_2O_2S impurity phase was observed. The refined lattice constant for the La_2O_2S phase was $a = 4.047(2)\,\text{Å}$ and $c = 6.944(3)\,\text{Å}$ for $x = 0$ and $a = 4.0498(6)\,\text{Å}$ and $c = 6.9502(9)\,\text{Å}$, which is consistent with the known value for La_2O_2S with a space group of $P\text{-}3m1$). In addition, very small impurity peaks due to PbO, $Pb_2Bi_2Ch_5$, and/or $PbBi_2Ch_4$ were observed. The impurity phase did not disappear when heat treatment conditions were changed. Therefore, we have investigated crystal structure and physical properties of the system with multi-phase samples. We performed two-phase Rietveld analyses to determine lattice constants for all the obtained samples. For convenience in the superconducting property part, we mention the characteristics of the impurity phases incorpolated in the examined samples. La_2O_2S and PbO is insulators. $Pb_2Bi_2Ch_5$, and $PbBi_2Ch_4$ are semiconductors with Pb^{2+} and Bi^{3+}. Although a band gap of these phases could be modified by the Se concentration of the Ch site, these systems should be basically semiconducting. Using a database (SuperCon, NIMS database: `https://supercon.nims.go.jp/`), we have checked that those compositions are not superconducting.

The results of the Rietveld refinement are summarized in table 1. The lattice constants a and c increase with Se substitution for $x = 0.5$, but the lattice constants for $x = 1.0$ were comparable to those for $x = 0.5$. Those shifts in lattice constants are consistent with the observed peak shifts, as shown in fig. 1(b), (c). Based on such facts, we consider the solubility limit of Se in S to be less than $x = 1.0$. We have analyzed the actual compositions of

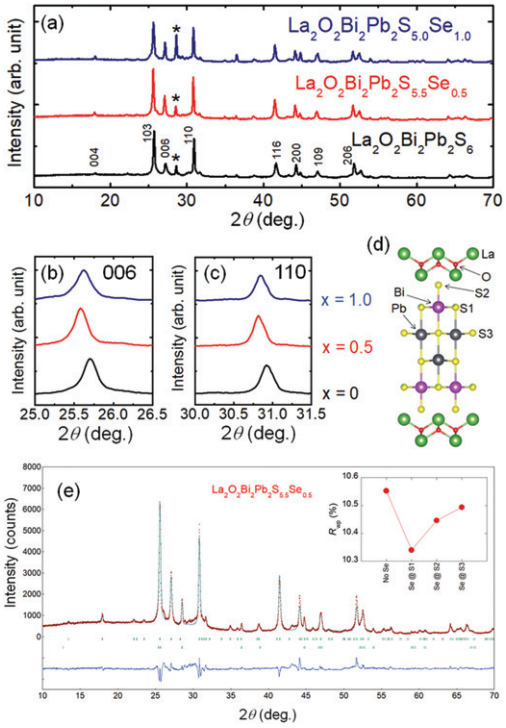

Fig. 1: (a) Powder XRD patterns for all the samples of $La_2O_2Bi_2Pb_2S_{6-x}Se_x$. The peak of the La_2O_2S impurity phase was indicated by an asterisk symbol. The numbers in the figures are Miller indices of typical peaks. (b) Zoomed profiles of 006 peaks. (c) Zoomed profiles of 110 peaks. (d) Schematic image of $La_2O_2Bi_2Pb_2S_{5.5}Se_{0.5}$ crystal structure drawn with parameters obtained from the Rietveld analysis. (e) Powder XRD pattern and the Rietveld fitting for the $La_2O_2Bi_2Pb_2S_{5.5}Se_{0.5}$ sample. The Rietveld analysis was performed by two-phase refinement with a La_2O_2S impurity phase as a second phase.

elements at the conducting layer in $La_2O_2Bi_2Pb_2S_{6-x}Se_x$ ($x = 0$, 0.5 and 1.0) by EDX analysis at five analysis points (table 1). The obtained compositions for the sample are almost the same as the initial nominal compositions, but the Se concentration for $x = 1.0$ is slightly lower than the nominal value. However, the Se concentrations were different for the samples with $x = 0.5$ and 1.0, and the superconducting property was also different. Therefore, for clarity to the readers, we labelled the samples according to the initial nominal compositions in this paper.

Figure 1(e) shows the result of Rietveld refinement for $x = 0.5$. To refine the XRD pattern for an Se-doped sample, we needed to determine the S site where Se is doped. The inset of fig. 1(e) shows the reliability factor (R_{wp}) obtained for the cases with no Se and those with Se-doped S1, S2, and S3 sites (see fig. 1(d) for the label of S sites). R_{wp} decreases with incorporation of Se at the S sites and becomes the lowest when Se substitution at the in-plane S1 site was assumed. Although we need further detailed structural parameters to draw firm conclusions regarding the Se-doping site, herein, we consider that Se was selectively substituted at the S1 site. This assumption is consistent with the emergence of metallic conductivity and superconductivity in Se-doped samples, which can be explained by the concept of in-plane chemical pressure via Se substitution at the S1 sites of BiS_2 layers [21–24,34].

Figure 2 shows the temperature dependence of the electrical resistivity ($\rho(T)$) from 300 to 2 K for $La_2O_2Bi_2Pb_2S_6$. The electrical resistivity largely increases with decreasing temperature, which in agreement with the typical behavior of semiconductors. The result is consistent with a previous report by Sun *et al.* [25]. However, the band calculation has suggested a metallic band structure for $La_2O_2Bi_2Pb_2S_6$ [26]. The inconsistency may imply that the semiconducting-like behavior of electrical resistivity is caused by anomalous carrier localization, not from characteristics of a band insulator.

Figure 3(a) shows the temperature dependence of electrical resistivity ($\rho(T)$) from 300 to 0.5 K for the Se-doped $La_2O_2Bi_2Pb_2S_{6-x}Se_x$ ($x = 0.5$ and 1.0) samples. At 300 K, the electrical resistivity is clearly lower than that of $La_2O_2Bi_2Pb_2S_6$. Furthermore, the semiconducting-like behavior was dramatically suppressed by Se substitution. The normal-state resistivity of Se-doped compounds still shows a slight increase with decreasing temperature, which may be due to weak carrier localization, which is typically observed in BiS_2-based systems. The weak carrier localization seems to be suppressed with increasing Se concentration from $x = 0.5$ to $x = 1.0$. The changes in resistivity caused by Se substitution can be understood by the effects of in-plane chemical pressure, which was introduced previously. For two-layer–type $BiCh_2$-based compounds, it has been extensively demonstrated that in-plane chemical pressure effects successfully suppressed the in-plane local disorder of the conducting layer [14,21–24,34]. Thus, we consider that the semiconducting-like behavior observed for $x = 0$ and the weak localization behavior observed for Se-doped samples are both related to the presence of local disorders in the BiS_2 layers in $La_2O_2Bi_2Pb_2S_{6-x}Se_x$. To investigate the local disorder, precise estimation of the displacement parameters using synchrotron X-ray diffraction or X-ray absorption spectroscopy, or single-crystal structural analysis. So far, we have not succeeded in the growth of single crystals or single-phase polycrystalline samples of $La_2O_2Bi_2Pb_2S_{6-x}Se_x$, which can be used for the investigation on the local disorder. Therefore, the scenario of the suppression of localized carriers is based on the analogy to the cases of BiS_2-based systems, in which huge displacements of in-plane atoms caused by the presence of Bi lone pairs were suppressed by Se substitution for the in-plane S site (in-plane chemical pressure effect).

We observed superconductivity in both the Se-doped samples, as shown in fig. 3(b), which is the zoomed view of fig. 3(a) near the superconducting transition region. T_c increases with increasing Se concentration in $La_2O_2Bi_2Pb_2S_{6-x}Se_x$. The zero-resistivity T_c (T_c^{zero}) is 1.2 K for $x = 0.5$ and 1.9 K for $x = 1.0$. Thus far, superconductivity in $La_2O_2Bi_2M_2S_6$ has been observed for $La_2O_2Bi_3AgS_6$-based compounds [30–33]. $La_2O_2Bi_3AgS_6$

Table 1: Rietveld analysis results, lattice constants, reliability factor R_{wp}, and mass fraction of the major phase to the impurity phase in $La_2O_2B_2Pb_2S_{6-x}Se_x$ ($x = 0$, 0.5, and 1.0).

Sample label	$La_2O_2Bi_2Pb_2S_6$ ($x = 0$)	$La_2O_2Bi_2Pb_2S_{5.5}Se_{0.5}$ ($x = 0.5$)	$La_2O_2Bi_2Pb_2S_{5.0}Se_{1.0}$ ($x = 1.0$)
a (Å)	4.0920(4)	4.1039 (3)	4.1038 (4)
c (Å)	19.680(2)	19.7642 (14)	19.777 (2)
R_{wp}	12.8%	10.5%	11.7%
Mass fraction of the main phase to La_2O_2S	95%	95%	82%
Actual composition (EDX)	$Bi_{1.98(3)}Pb_{2.09(8)}S_{6.04(9)}$	$Bi_{2.01(3)}Pb_{1.89(5)}S_{5.52(8)}Se_{0.46(3)}$	$Bi_{2.04(1)}Pb_{1.95(2)}S_{5.18(5)}Se_{0.81(10)}$

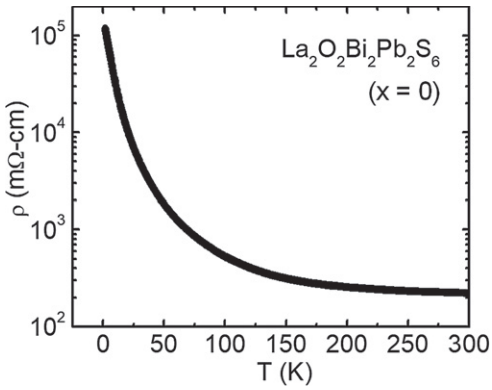

Fig. 2: Temperature (T) dependence of electrical resistivity ($\rho(T)$) from 300 K to 2 K for $La_2O_2Bi_2Pb_2S_6$.

exhibits metallic conductivity without Se substitution but shows a CDW-like (charge density wave-like) anomaly in $\rho(T)$. Although the origin of the anomaly has not been clarified, it could be related to the anomalous insulating behavior observed in $La_2O_2Bi_2Pb_2S_6$. The emergence of metallic conductivity and superconductivity via Se substitution in $La_2O_2Bi_2Pb_2S_{6-x}Se_x$ could provide us with important information for the further development of four-layer–type Bi-based superconductors.

Figures 4(a) and (b) show the temperature dependence of electrical resistivity under various magnetic fields ($\rho(T, B)$) for $La_2O_2Bi_2Pb_2S_{6-x}Se_x$ ($x = 0.5$ and 1.0). T_c shifts towards a lower temperature with an increase in the magnetic field. We observed an onset drop in the resistivity due to the superconductivity even at $B = 2$ T for $x = 1.0$. The T_c onset shifts gradually with an increasing magnetic field as opposed to the shift in T_c^{zero}, which is the characteristic behavior of layered superconductivity against the magnetic field. The magnetic field-temperature phase diagrams are plotted in fig. 4(c). The upper critical fields are estimated based on the temperature where resistivity becomes 90% of the normal-state resistivity near T_c. The upper critical field $B_{c2}(T)$ at absolute zero temperature, $B_{c2}(0)$,

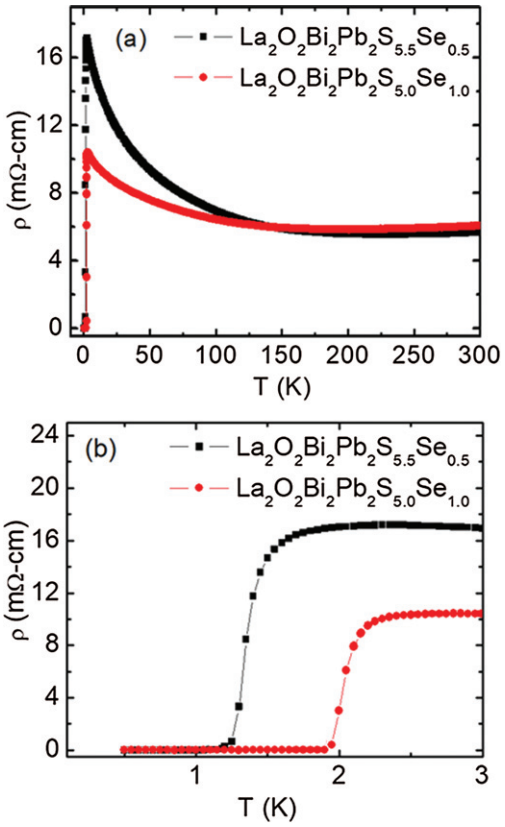

Fig. 3: (a) Temperature dependence of electrical resistivity from 300 to 0.5 K for $La_2O_2Bi_2Pb_2S_{6-x}Se_x$ ($x = 0.5$ and 1.0). (b) $\rho(T)$ curve in the temperature range 3.0–0.5 K.

is analyzed using the conventional one-band Werthamer-Helfand-Hohenberg (WHH) equation [42], which gives $B_{c2}(0) = -0.693 T_c (dB_{c2}/dT)_{T=T_c}$. $B_{c2}(0)$ is 0.76 and 1.15 T for $x = 0.5$ and 1.0, respectively.

To investigate the changes in carrier concentration, Seebeck coefficient (S) and Hall coefficient (R_H) were measured for $La_2O_2Bi_2Pb_2S_{6-x}Se_x$. Although the samples contain a La_2O_2S impurity phase and tiny amount of PbO and Pb-Bi-Ch phases, we consider that we can qualitatively analyze the changes in carrier concentration

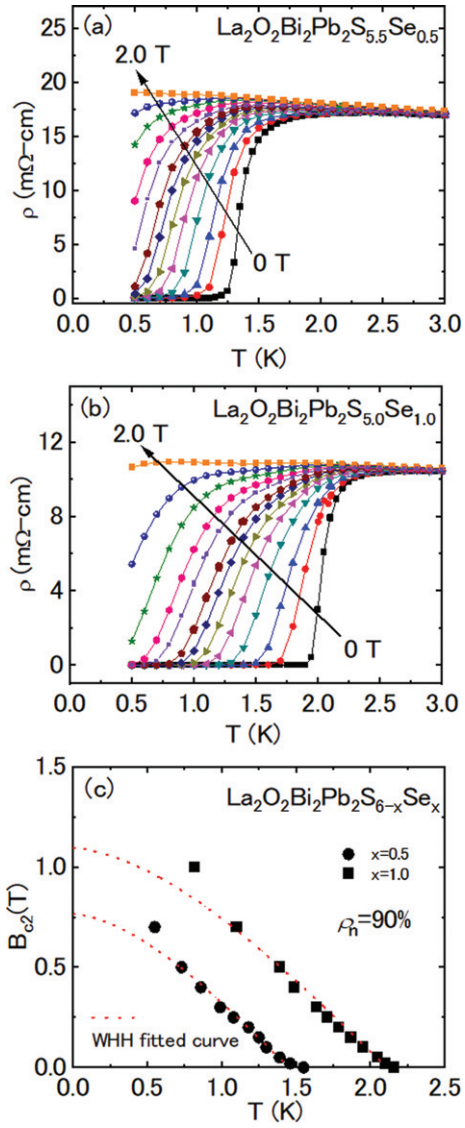

Fig. 4: (a, b) Temperature dependence of electrical resistivity from 3.0 to 0.5 K for $La_2O_2Bi_2Pb_2S_{6-x}Se_x$ ($x = 0.5$ and 1.0) under magnetic fields. (c) Temperature dependence of $B_{c2}(T)$ for $La_2O_2Bi_2Pb_2S_{6-x}Se_x$ ($x = 0.5$, and 1.0). The points with different symbols represent experimental data and the dotted lines represent fitting curves as per the WHH theory.

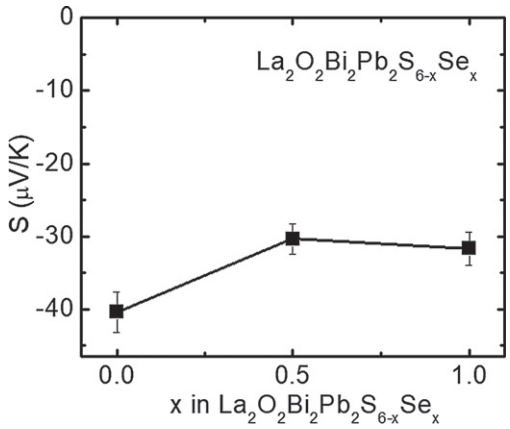

Fig. 5: The x dependence of Seebeck coefficient for $La_2O_2Bi_2Pb_2S_{6-x}Se_x$ at room temperature.

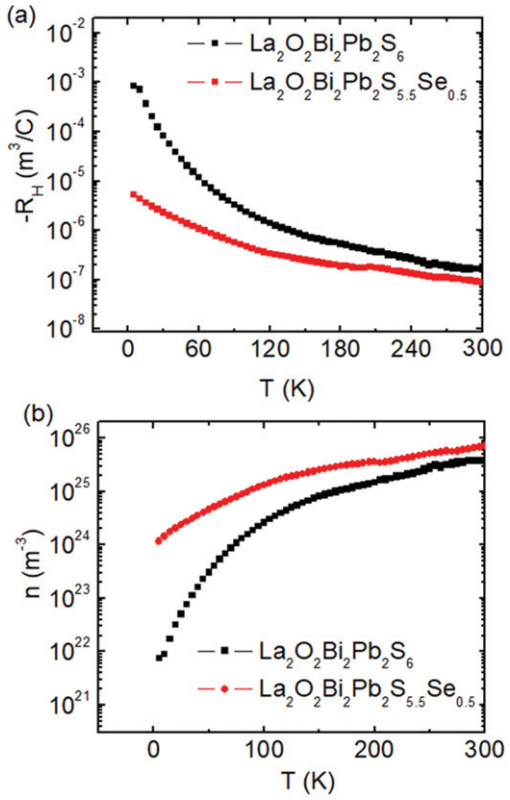

Fig. 6: (a) Temperature dependence of Hall coefficient (R_H) for $La_2O_2Bi_2Pb_2S_{6-x}Se_x$ ($x = 0$ and 0.5) under the magnetic field of 9 T. (b) Temperature dependence of estimated carrier concentration for $La_2O_2Bi_2Pb_2S_{6-x}Se_x$ ($x = 0$ and 0.5).

or mobility by Se substitution. As shown in fig. 5, the Seebeck coefficient is negative, which indicates that the dominant carriers are electrons. The absolute value of S decreases from $x = 0$ to $x = 0.5$. Seebeck coefficient for $x = 0.5$ and 1.0 is almost the same. From the results, we can roughly estimate that the carrier concentration slightly increased by Se substitution. Figure 6(a) shows the temperature dependence of Hall coefficient ($-R_{\rm H}$) from 2 K to 300 K under the fixed magnetic field of 9 T for $La_2O_2Bi_2Pb_2S_{6-x}Se_x$ ($x = 0$ and 0.5). Hall coefficients are all negative, which is consistent with the results of Seebeck coefficient, but $-R_{\rm H}$ for $x = 0.5$ is largely suppressed as compared to that for $x = 0$. To investigate the carrier density we have used the simple single band modle $n = |1/eR_{\rm H}|$, where n is the charge carrier density and e is the electron charge, as demonstrated for other layered Bi-based compounds [25,43,44]. Figure 6(b) shows the temperature dependences of electron carrier density for $La_2O_2Bi_2Pb_2S_{6-x}Se_x$ ($x = 0$ and 0.5), which suggests that the carriers density increases by Se substitution. Having considered the valence state of S and Se, which

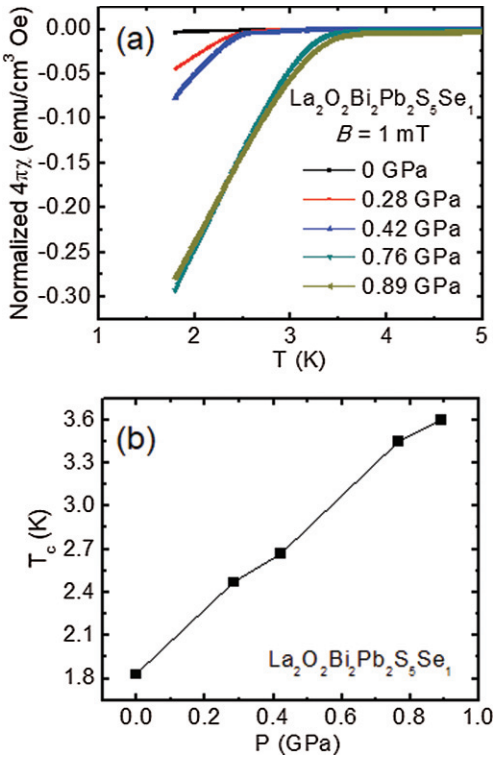

Fig. 7: (a) Temperature dependences of magnetic susceptibility $4\pi\chi$ under high pressure for $x = 1.0$. (b) Pressure dependence of T_c for $x = 1.0$.

is considered as -2 for both, we do not expect a huge change in carrier concentration. Thus, the huge increase in carrier density may be related to the in-plane chemical pressure effects. As a fact, metalicity has been induced by Se substitution. From those facts, we consider that the huge change in carrier concentration estimated here is related to the increase in the concentration of *mobile* carrier. With this assumption, low carrier density for $x = 0$ can be considered as resulting from carrier localization due to the local disorder in the BiS_2 layers.

To investigate the bulk nature of the superconductivity, we have performed magnetic susceptibility measurements for $x = 1.0$, but a large shielding signals could not be due to the low T_c of 1.9 K, which is close to the temperature limit of our SQUID system, 1.8 K. Therefore, we have performed susceptibility measuremetns under high pressure. Figure 7(a) shows the temperature dependences of normalized susceptibility $4\pi\chi$ under high pressure. (The data was normalized at 6 K because superconducting signals of Pb manometor is detected above 6 K.) T_c increased with increasing pressure and reached 3.6 K at 0.89 GPa. Large shielding signals are observed. T_c estimated from the susceptibility drop in fig. 7(a) is plotted in fig. 7(b) as a function of pressure. The improvement of superconducting properties of $x = 1.0$ by external pressure effect is basically consistent with the above in-plane chemical pressure effect by Se substitution. In BiS_2-based systems, both external pressure and chemical pressure improved superconducting properties [4,5,34,45]. Both pressure effects modif an in-plane crystal structure. To further investigate the effect of external and/or chemical pressure to the crystal structure and superconducting properties of the $La_2O_2Bi_2Pb_2S_{6-x}Se_x$ system, local structure analyses under high pressure are needed.

Conclusion. – $La_2O_2Bi_2Pb_2S_6$ is a four-layer–type Bi-based compound that shows insulating transport properties at low temperatures. Hence, in this study, we have investigated the effects of Se substitution on the structural, transport, and superconducting properties of $La_2O_2Bi_2Pb_2S_{6-x}Se_x$. Owing to Se doping, the normal state electrical resistivity at low temperatures was drastically suppressed, and superconductivity at a transition temperature (T_c) of 1.2 K was observed for $x = 0.5$. T_c increased with increasing Se concentration: $T_c = 1.9$ K for $x = 1.0$. According to XRD analyses, we proposed that Se was substituted for the in-plane S1 site in the BiS_2 layers. Both the Seebeck coefficient and the Hall coefficient suggested that electrons were the dominant carriers. From the Hall coefficient, carrier concentration was estimated. Owing to Se substitution, the concentration of mobile carriers increased considerably; this could be related to the suppression of carrier localization caused by Se substitution. On the basis of the obtained results and the discussion based on the analogy of two-layer–type systems, the emergence of metallicity and superconductivity was explained by the in-plane chemical pressure effects. The estimated $B_{c2}(0)$ was 0.76 and 1.15 T for $x = 0.5$ and 1.0, respectively. By applying high pressure for $x = 1.0$, bulk superconductivity was confirmed and the T_c increased up to 3.6 K at 0.89 GPa. The demonstration of metallicity and superconductivity in $La_2O_2Bi_2Pb_2S_6$-based compounds can be useful for further development of four-layer–type Bi-based superconductors.

* * *

This work was partly supported by grants in Aid for Scientific Research (KAKENHI) (Grant Nos. 15H05886, 15H05884, 16H04493, 18KK0076, and 15H03693) and the Advanced Research Program under the Human Resources Funds of Tokyo (Grant No. H31-1).

REFERENCES

[1] Bednorz J. G. and Muller K. A., *Z. Phys. B*, **64** (1986) 189.
[2] Kamihara Y., Watanabe T., Hirano M. and Hosono H., *J. Am. Chem. Soc.*, **130** (2008) 3296.
[3] Mizuguchi Y., Fujihisa H., Gotoh Y., Suzuki K., Usui H., Kuroki K., Demura S., Takano Y., Izawa H. and Miura O., *Phys. Rev. B*, **86** (2012) 220510(R).
[4] Mizuguchi Y., Demura S., Deguchi K., Takano Y., Fujihisa H., Gotoh Y., Izawa H. and Miura O., *J. Phys. Soc. Jpn.*, **81** (2012) 114725.

[5] Mizuguchi Y., *J. Phys. Soc. Jpn.*, **88** (2019) 041001.

[6] Barišić N., Chan M. K., Li Y., Yu G., Zhao X., Dressel M., Smontara A. and Greven M., *Proc. Natl. Acad. Sci. U.S.A.*, **110** (2013) 12235.

[7] Ishida K., Nakai Y. and Hosono H., *J. Phys. Soc. Jpn.*, **78** (2009) 062001.

[8] Mizuguchi Y. and Takano Y., *J. Phys. Soc. Jpn.*, **79** (2010) 102001.

[9] Demura S., Mizuguchi Y., Deguchi K., Okazaki H., Hara H., Watanabe T., Denholme S. J., Fujioka M., Ozaki T., Fujihisa H., Gotoh Y., Miura O., Yamaguchi T., Takeya H. and Takano Y., *J. Phys. Soc. Jpn.*, **82** (2013) 033708.

[10] Jha R., Kumar A., Singh S. K. and Awana V. P. S., *J. Supercond. Nov. Magn.*, **26** (2013) 499.

[11] Xing J., Li S., Ding X., Yang H. and Wen H. H., *Phys. Rev. B*, **86** (2012) 214518.

[12] Yazici D., Huang K., White B. D., Chang A. H., Friedman A. J. and Maple M. B., *Philos. Mag.*, **93** (2012) 673.

[13] Yazici D., Huang K., White B. D., Jeon I., Burnett V. W., Friedman A. J., Lum I. K., Nallaiyan M., Spagna S. and Maple M. B., *Phys. Rev. B*, **87** (2013) 174512.

[14] Kajitani J., Deguchi K., Hiroi T., Omachi A., Demura S., Takano Y., Miura O. and Mizuguchi Y., *J. Phys. Soc. Jpn.*, **83** (2014) 065002.

[15] Lin X., Ni X., Chen B., Xu X., Yang X., Dai J., Li Y., Yang X., Luo Y., Tao Q., Cao G. and Xu Z., *Phys. Rev. B*, **87** (2013) 020504(R).

[16] Zhai H. F., Tang Z. T., Jiang H., Xu K., Zhang K., Zhang P., Bao J. K., Sun Y. L., Jiao W. H., Nowik I., Felner I., Li Y. K., Xu X. F., Tao Q., Feng C. M., Xu Z. A. and Cao G. H., *Phys. Rev. B*, **90** (2014) 064518.

[17] Zhai H. F., Zhang P., Wu S. Q., He C. Y., Tang Z. T., Jiang H., Sun Y. L., Bao J. K., Nowik I., Felner I., Zeng Y. W., Li Y. K., Xu X. F., Tao Q., Xu Z. A. and Cao G. H., *J. Am. Chem. Soc.*, **136** (2014) 15386.

[18] Jha R., Tiwari B. and Awana V. P. S., *J. Phys. Soc. Jpn.*, **83** (2014) 063707.

[19] Krzton-Maziopa A., Guguchia Z., Pomjakushina E., Pomjakushin V., Khasanov R., Luetkens H., Biswas P., Amato A., Keller H. and Conder K., *J. Phys.: Condens. Matter*, **26** (2014) 215702.

[20] Li L., Xiang Y., Chen Y., Jiao W., Zhang C., Zhang L., Dai J. and Li Y., *Supercond. Sci. Technol.*, **29** (2016) 04LT03.

[21] Wang X. C., Chen D. Y., Guo Q., Yu J., Ruan B. B., Mu Q. G., Chen G. F. and Ren Z. A., arXiv:1404.7562.

[22] Jinno G., Jha R., Yamada A., Higashinaka R., Matsuda T. D., Aoki Y., Nagao M., Miura O. and Mizuguchi Y., *J. Phys. Soc. Jpn.*, **85** (2016) 124708.

[23] Goto Y., Sogabe R. and Mizuguchi Y., *J. Phys. Soc. Jpn.*, **86** (2017) 104712.

[24] Sogabe R., Goto Y., Nishida A., Katase T. and Mizuguchi Y., *EPL*, **122** (2018) 17004.

[25] Sun Y.-L., Ablimit A., Zhai H.-F., Bao J.-K., Tang Z.-T., Wang X.-B., Wang N.-L., Feng C.-M. and Cao G.-H., *Inorg. Chem.*, **53** (2014) 11125.

[26] Mizuguchi Y., Hijikata Y., Abe T., Moriyoshi C., Kuroiwa Y., Goto Y., Miura A., Lee S., Torii S., Kamiyama T., Lee C. H., Ochi M. and Kuroki K., *EPL*, **119** (2017) 26002.

[27] Hijikata Y., Abe T., Moriyoshi C., Kuroiwa Y., Goto Y., Miura A., Tadanaga K., Wang Y., Miura O. and Mizuguchi Y., *J. Phys. Soc. Jpn.*, **86** (2017) 124802.

[28] Wu M. K., Ashburn J. R., Torng C. J., Hor P. H., Meng R. L., Gao L., Huang Z. J., Wang Y. Q. and Chu C. W., *Phys. Rev. Lett.*, **58** (1987) 908.

[29] Maeda H., Tanaka Y., Fukutomi M. and Asano T., *Jpn. J. Appl. Phys.*, **27** (1988) L209.

[30] Jha R., Goto Y., Higashinaka R., Matsuda T. D., Aoki Y. and Mizuguchi Y., *J. Phys. Soc. Jpn.*, **87** (2018) 083704.

[31] Jha R., Goto Y., Matsuda T. D., Aoki Y., Nagao M., Tanaka I. and Mizuguchi Y., *Sci. Rep.*, **9** (2019) 13346.

[32] Jha R., Goto Y., Higashinaka R., Miura A., Moriyoshi C., Kuroiwa Y. and Mizuguchi Y., arXiv:1908.09311.

[33] Kim G. C., Cheon M., Choi W., Ahmad D., Kwon Y. S., Ko R. and Kim Y. C., *J. Supercond. Nov. Magn.*, **33** (2020) 625.

[34] Mizuguchi Y., Miura A., Kajitani J., Hiroi T., Miura O., Tadanaga K., Kumada N., Magome E., Moriyoshi C. and Kuroiwa Y., *Sci. Rep.*, **5** (2015) 14968.

[35] Paris E., Joseph B., Iadecola A., Sugimoto T., Olivi L., Demura S., Mizuguchi Y., Takano Y., Mizokawa T. and Saini N. L., *J. Phys.: Condens. Matter*, **26** (2014) 435701.

[36] Mizuguchi Y., Paris E., Sugimoto T., Iadecola A., Kajitani J., Miura O., Mizokawa T. and Saini N. L., *Phys. Chem. Chem. Phys.*, **17** (2015) 22090.

[37] Athauda A., Yang J., Lee S., Mizuguchi Y., Deguchi K., Takano Y., Miura O. and Louca D., *Phys. Rev. B*, **91** (2015) 144112.

[38] Nagasaka K., Nishida A., Jha R., Kajitani J., Miura O., Higashinaka R., Matsuda T. D., Aoki Y., Miura A., Moriyoshi C., Kuroiwa Y., Usui H., Kuroki K. and Mizuguchi Y., *J. Phys. Soc. Jpn.*, **86** (2017) 074701.

[39] Mizuguchi Y., Hoshi K., Goto Y., Miura A., Tadanaga K., Moriyoshi C. and Kuroiwa Y., *J. Phys. Soc. Jpn.*, **87** (2018) 023704.

[40] Izumi F. and Momma K., *Solid State Phenom.*, **130** (2007) 15.

[41] Momma K. and Izumi F., *J. Appl. Crystallogr.*, **41** (2008) 653.

[42] Werthamer N. R., Helfand E. and Hohenberg P. C., *Phys. Rev.*, **147** (1966) 295.

[43] Pallecchi I., Lamura G., Putti M., Kajitani J., Mizuguchi Y., Miura O., Demura S., Deguchi K. and Takano Y., *Phys. Rev. B*, **89** (2014) 214513.

[44] Nishida A., Nishiate H., Lee C. H., Miura O. and Mizuguchi Y., *J. Phys. Soc. Jpn.*, **85** (2016) 074702.

[45] Tomita T., Ebata M., Soeda H., Takahashi H., Fujihisa H., Gotoh Y., Mizuguchi Y., Izawa H., Miura O., Demura S., Deguchi K. and Takano Y., *J. Phys. Soc. Jpn.*, **83** (2014) 063704.